

Protection of Ultrasound Image Sequence: Employing Motion Vector Reversible Watermarking

Rafi Ullah Habib¹, Fayez Al-Fayez²

Department of Computer Science and Information
College of Science, Majmaah University
Majmaah 11952, Saudi Arabia

Abstract—In healthcare information systems, medical data is very important for diagnosis. Most of the health institutions store their patients' data on third-party servers. Therefore, its security is very important, since the advent of advanced multimedia and communication technology, whereby digital contents are manipulated, copied, and duplicated without leaving any trace. In this paper, a reversible watermarking technique is applied to the patients' data (ultrasound image sequence). Since the traditional watermarking schemes can experience some permanent distortions that are not acceptable in the medical application. Thus, a reversible watermarking technique has been used, which can not only secure the ultrasound image sequence but also restore the original sequence back. For watermark embedding, the magnitude and phase angles of motion vectors of the image sequence are used that are obtained by using Full-Search block-based motion estimation algorithm. Before applying the motion estimation algorithm and watermark embedding, the histogram pre-processing is performed to avoid underflow/overflow. Unlike other state-of-the-art watermarking schemes that are reported in the last decades, the experimental results show that the proposed algorithm is simple, provides a much larger embedding capacity and better quality of the watermarked image sequence.

Keywords—Reversible watermarking; ultrasound sequence; full-search; motion vectors; side information

I. INTRODUCTION

Due to advances in the generation, communication and storage of the digital data, its security has gained the immense importance in multimedia applications and services. Medical images are more critical, where the use of manipulated images are more dangerous and can be life-threatening [1, 2]. Thus, the reliability of digital image/sequences, especially medical image/sequences is an open challenge for the researchers and Hospital Information Management Systems (HIMS). HIMS demands secure storage and transmission of the patient data where the end-user cannot tolerate a risk to get the distorted information. In such a scenario, simple watermarking methods are not feasible and hence a reversible watermarking is much needed, where the original content can be restored and the doctors can evaluate the unmodified data. In this paper, a motion vector reversible watermarking scheme has been introduced that is able to secure the ultrasound image sequence with improved imperceptibility and capacity. Although, reversible watermarks contain a large number of bits. However, in the proposed work, it does not affect the visual perception of the video.

The ultrasound videos have a vital role in the medical diagnostic system. For example, in [3], the authors have proposed an accurate classification model for stratification of liver disease in ultrasound. Watermarking using machine learning and bio-inspired algorithms are also used for the security of the digital contents [4]. Several critical parameters like visual perception, capacity, robustness, and security level, are to be considered while using the idealized watermarking system. For still images, the watermark(s) can be embedded in the spatial and frequency domain. For, images sequence, the temporal domain can be used, where the watermark(s) can be embedded in the estimated motion (motion vectors). The basic requirements for medical image watermarking are fidelity, robustness, imperceptibility, security, capacity, computational complexity, reliability, and reversibility [5]. Usually the distortion is visible but still, it is not acceptable when the exact genuine content is critical like the military and medical applications. To avoid such type of problem, a reversible watermarking has been used since last two decades, which have the ability to not only protect the digital content by embedding an assigned watermark but also recover the original content back. There are three major categories of reversible watermarking schemes as presented in [1]: compression-based reversible watermarking, histogram-based reversible watermarking and difference-expansion (DE) based reversible watermarking. In the above-mentioned categories, the compression based reversible watermarking is computationally complex and has limited embedding capacity. However, the remaining two methods are simple and provide high capacity for embedding the reversible watermark, which contains some side information along with the watermark bits. Several reversible watermarking algorithms have been developed in the last decade for protecting the images as well as videos [6 - 9].

Rest of the paper is organized as follow: Details of the current work about reversible watermarking are discussed in Section II. Short descriptions of motion estimation algorithms are discussed in Section III. The proposed watermark embedding and extraction procedures are presented in Section IV. Experimental and conclusions are presented in Section V and Section VI respectively. In Section VII, the research contributions and limitations are discussed.

II. LITERATURE REVIEW

Since the last three decades, digital watermarking has been used for protecting all types of media content like images, audio, videos and other printed materials, and documents.

Digital watermarking is used in many applications like military, medical, remote sensing, surveillance etc. Several reversible watermarking schemes have been designed for different applications.

In 2011, a reversible video watermarking scheme using motion vectors and prediction error expansion has been proposed by X. Zeng et.al [10]. The relationship between neighbouring frames and prediction errors are explored that significantly sharpen the distribution of prediction errors. Then histogram-modification is utilized for expanding the prediction errors. Due to the minor modification of pixel values, the video quality is preserved. In the phase angles of motion vectors and histogram modification, a little side information is generated that is combined with the pure watermark and then embedded in the video. The algorithm is tested on four different normal videos like Salesman, Foreman, Grandmother, Trevor, where unlike the normal videos, the medical image sequence has more capacity for embedding.

In [11], Diljit et al. proposed a reversible watermarking based on shifting histogram. The authors proposed a method to improve the imperceptibility and mitigate the capacity control problem. They also proposed the reversible watermark embedding based on prediction-error expansion. Similarly, Caldelli et al. present an overview of the reversible watermarking that is appeared in five years duration (from 2005 to 2010) [12].

In [13], a bi-directional video watermarking has been proposed. The authors have multiple scan images as watermarks and the same are trained by bi-directional associative memory (BAM) neural network. Its performance is evaluated with different kind of geometric and video processing attacks. The imperceptibility is about 50dB and the robustness is 1.0 in terms of normalized cross-correlation (NCC).

Loganathana and Kaliyaperumal proposed an HVS based video watermarking using BAM neural network and fuzzy inference system [14]. They are focusing on the robustness of the video for secure transmission over communication channels. The weight matrix is generated and embedded in the wavelet coefficients of all components of all frames. Fuzzy inference system takes the HVS characteristics as an input in the wavelet transform. Imperceptibility is 60 dB and the robustness is 1.0 in terms of NCC. Similarly, Agilandeewari and Ganesan proposed an optimal quaternion curvelet transform (QCT) based video watermarking [15]. They improve the three contradictory properties of watermarking; imperceptibility, robustness and security to the most notable attacks i.e. geometric attacks and image and video processing attacks.

In [16], DWT (discrete wavelet transform) based intravascular ultrasound video watermarking has been proposed. The ultrasound sequence is split into frames and applications of DWT; DCT (discrete cosine transforms) followed by Singular Value Decomposition (SVD) composes the watermark embedding technique and obtain an imperceptible watermarked video. The inverse of the above transformations is applied to the extraction side.

In 2014, an intelligent reversible watermarking technique in medical images using Genetic Algorithms (GA) and Particle Swarm Optimization (PSO) has been proposed by Naheed et.al. [17]. In this scheme, the authors have focused on the applications where the high embedding capacity and imperceptibility is required to maintain the reliability of the host content as well as embedded information. In this scheme, the authors are focusing on improving the imperceptibility and embedding capacity. The authors study the Luo's [8] additive interpolation error expansion scheme and enhanced it by incorporating with two popular intelligent techniques: GA and PSO. The better estimation of neighbouring pixel values is obtained by applying GA, exploiting the correlation of image pixel values, which results in an optimal balance between and imperceptibility and embedding capacity.

In 2014, B. Lie et.al [18] proposed a reversible watermarking algorithm for protecting medical images. The authors used differential evolution (DE) based watermarking. After applying the wavelet transformation and singular value decomposition (SVD), the textual data and signature information are embedded in the original medical images using recursive dither modulation (RDM) method. In addition, the strength of the watermark is optimally controlled by applying DE to design the quantization steps (QSs). This scheme is able to get better results in terms of the contradicting properties of watermarking i.e. imperceptibility and robustness.

In 2014, S. Acharjee et.al [19] proposed the watermarking scheme to protect medical image sequences based on motion estimation. The original image is watermarked inside the motion estimation of two consecutive frames of an echocardiograph video/image-sequence. The ultrasound images sequence has been used as test data. The correlation between the original and cover work has been calculated. In addition, SSIM (structural similarity index measure) and (PSNR (peak signal to noise ratio) are used to check the distortion and structural similarity between the original and the watermarked frame respectively.

In 2014, H. Yeh et.al, [20] proposed the watermarking algorithm for videos using the neighbouring similarity. Prediction encoding has been employed to compute the prediction errors and then all of the prediction errors are explored to develop a histogram-based reversible video watermarking algorithm. This algorithm has been tested on many images. Capacity and PSNR are calculated. For different block sizes, it gives different capacities and PSNRs. The PSNRs are around 51dB, which is much better for normal images and applications.

Reversible watermarking scheme for videos using motion vectors has been proposed in 2017 [21]. An efficient reversible watermark embedding method, based on the histogram based shifting, has been proposed. By designating, specific decoded reference frames, the distortion accumulation effects due to modification of the motion vectors have been overcome. All the extracted information can be recovered without loss of the original compressed video carrier.

In 2017, Arsalan et al. [22] has proposed the intelligent reversible watermarking scheme for protecting medical images. In this scheme, the embedding distortion has been reduced by

exploiting the concept of companding function. An integer wavelet transform has been used as an embedding domain for achieving reversibility of the host images. To avoid underflow and/or overflow, histogram processing is employed. In addition, for selecting the suitable coefficients for embedding watermark bits, the learning capabilities of genetic programming (GP) has been utilized. GP model is evolved that not only make an optimal tradeoff between the contradicting properties of watermarking i.e. imperceptibility and capacity but also exploit the wavelet coefficient hidden dependencies and information related to the type of subband.

A recursive histogram-based reversible video watermarking has been proposed by Vural and Yildirim in 2017 [23]. The algorithms are based on motion compensated interpolation or prediction error expansion. A recently developed recursive-histogram based reversible watermarking has been utilized for embedding the watermark bits in the motion compensated interpolation. In reversible video watermarking, the recursive histogram modification cannot be applied directly. Because ensuring the reversibility of each frame and distribution of total capacity among frames are encountered.

III. MOTION ESTIMATION ALGORITHMS

In literature, several block-matching algorithms for extracting the motion vectors are discussed in detail. Short descriptions of some of them are as follows.

A. Exhaustive Search/Full Search (ES/FS)

FS has a high computational cost because of its point selection in the selected window. In this BMA, for each non-overlapping blocks of the current frame, the reference frame is searched within the whole search space to find out the closest match. As the accuracy of motion vectors is focused, the FS method is used for obtaining the motion vectors [24].

B. Three-Step Search (TSS)

It is simple, robust, and near to optimality but its disadvantage is the uniform allocation of checkpoint patterns in the first step, where eight blocks around the centre block with fixed step size are selected for comparison. TSS is not efficient for small motions in a video [25].

C. New Three-Step Search (NTSS)

NTSS overcome the problem of small motion. It employs the centre-biased checkpoint pattern in the first step. NTSS yields better results than TSS and computational complexity is reduced by halfway search. NTSS is normally used for MPEG-1 and H.261 [26].

D. Four-Step Search (FSS)

In four-step search, a nine-point comparison is introduced, that starts with a step size of two and the selection of nine points around the search window. The distortion is calculated at each point and the points having the smallest distortion are selected [27].

E. Diamond Search (DS)

This BMA is similar to FSS, but the search point pattern is diamond-shaped rather than square. DS has two variants: large

and small DS patterns. The performance of DS is the same as that of NTSS, but its computational cost is lower [28].

F. Two-Dimensional Logarithmic Search (TDLS)

TDLS requires more steps than TSS but is more accurate with the large search window. It selects an initial step size and examines the central block and the four blocks at some predefined distance from the central block. If the best match is found, the step size is halved. This process continues until the step size reaches one [29].

G. Orthogonal Search Algorithm (OSA)

It is a combination of TSS and TDLS. The two points at a predefined distance from the centre of the search space in a horizontal direction are examined to determine for least distortion [30].

Comparative analysis of the performance of the BMAs discussed in this section, are given in Table I. The worst-case complexity is given in the second column, where the symbol p represents the search point. It is important to compare BMAs in order to identify which is most suitable for a given application.

IV. PROPOSED METHOD

A reversible watermarking approach has been developed for the security of ultrasound image sequence. Motion estimation is employed to process the ultrasound sequence to improve the capacity, imperceptibility and robustness. MATLAB environment is used for the experimental work. All the results are obtained by using MATLAB (2016a) running on Intel core i5, with 4GB RAM. The details of the ultrasound sequence are given in Table VII [31].

TABLE I. COMPARATIVE PERFORMANCE OF COMMON BMAS

| BMA | Computational Complexity | Advantages | Disadvantages |
|-------|--------------------------------|---|--|
| ES/FS | $(2 * p + 1)^2$ | Gives the best frame match and highest PSNR. | Computational cost is high. |
| TSS | $[1 + 8 \log 2(p + 1)]$ | Low complexity and optimal performance. Best for MPEG2. | Cannot detect small motions. |
| NTSS | $[1 + 8 \log 2(p + 1)] + 8$ | Efficient for small motions compared to TSS in terms of complexity. | More complex than TSS for large motion vectors. |
| FSS | $(18 \log 2[(p + 1) / 4] + 9)$ | Efficient for small motions by reducing the initial step size. | More complex than TSS. |
| DS | | Better than FSS in terms of MSE and search points. | Similar to NTSS. |
| TDLS | $[1 + 6 \log 2(p + 1)]$ | Fewer complexes than TSS. uses MSE distance criterion. | Only suitable for texture-dominated pictures. |
| OSA | $[1 + 4 \log 2(p + 1)]$ | Performs efficiently in terms of complexity as compared to TSS. | Very inefficient for small motions. Higher MSE than TSS. |

- A Full-search block-matching algorithm (BMA) is applied to the input ultrasound sequence to obtain the temporal information in the form of motion vectors. As compared to all other block-based motion estimation algorithms, a drawback of Full Search is its time-consumption. Full Search BMA is used because it is more efficient in terms of accuracy. Full-Search calculates the cost function at each point in the selected window and produces accurate motion vectors as compared to other BMAs. In this work, the accuracy is focused rather than computational cost.
- As compared to the common videos, medical image sequences like EEG topo-maps have more embedding capacity, thus it is easy to make a tradeoff between the contradictory parameters i.e. robustness, imperceptibility and embedding capacity.
- A binary watermark is generated first and then embedded in the motion vectors of the ultrasound sequence. The watermark carries the patient information along with the side information. By using the patient information as a watermark, a risk of a mismatch between the patient information and the associated image/video can be tackled easily. The side information is used to recover the original content back. The details of side information are given in Section 3.2.
- Based on the magnitude and phase angle, the suitable motion vectors are selected for watermark embedding. The selected motion vectors are called candidate motion vectors (CMVs). Although, it is not necessary that motion vectors having large magnitude are suitable for watermark embedding. However, it depends on the associated macroblock. We cannot rely directly on the magnitude of the vector and thus, the associated macroblock are focused parallelly.
- The effect of watermark embedding is checked by using PSNR and SSIM.

A. Watermark Embedding

To overcome the potential problem of overflow and underflow, histogram pre-processing is performed before embedding the watermark bits into the host data. A very simple example of histogram modification is explained in Fig. 1 [17]. The figure shows the original image and the modified image obtained after modifying the histogram. The range of the gray levels is 0–255, and following the histogram modification, the gray level range becomes 1–254. This is because after modification, the grayscale value 0 is replaced by grayscale value 1 and grayscale 1 is replaced by the grayscale value 2 and so on. Similarly, grayscale 255 is replaced by gray scale 254 and grayscale 254 is replaced by 253, and so on.

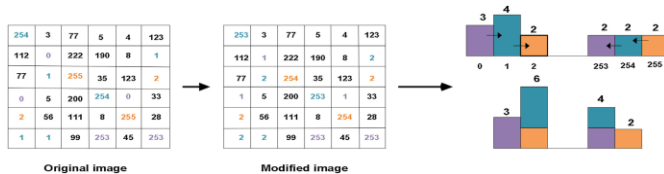


Fig. 1. Histogram of Original and Modified Images.

For reversibility, the frames of the ultrasound image sequence are embedded in the reverse order one-by-one. As shown in Fig. 3, the last frame is embedded first; the second last frame is embedded in next and so on until the first frame is embedded in the last. In the last frame, the only generated watermark bits are embedded where there is no information for reversibility. After this, some information used for extracting and recovering are recorded, such as motion vector and boundary map and is called side information. The details about the side information are given in Section 3.2. The side information is then combined with the watermark and embedded into the previous frame i.e. second last frame. This process continues until watermark bits along with the side information are embedded in the first frame [23]. The size of the side information is small and hence it will not affect the imperceptibility of the watermarked image sequence. The following procedure is followed for embedding the reversible watermark bits.

- 1) After performing the histogram pre-processing, the motion vectors are generated. Watermark is also generated and is ready for embedding in the suitable motion vectors.
- 2) Let we have the motion vector $MV_{i,j}$, where i is the i th frame and j is the j th motion vectors of the i th frame.
- 3) The horizontal and vertical components i.e. MV_x and MV_y are used for watermark embedding in the following manner.
- 4) The algorithm embeds the information in the ultrasound image sequence (video) in which reference frames is specified.
- 5) The vectors having greater magnitude from the selected threshold T , mean that it has fast moved other object. Assume that $S = \{MV_0, MV_1, MV_2, \dots, MV_{n-1}, \}$, $|S| = n$, where $|MV_i| \geq T, 0 \leq i < n$.
- 6) For each motion vector in S , the phase angle is computed $\theta = \tan^{-1}(MV_{iV}/MV_{iH})$, where $(MV_{iV}$ and MV_{iH} are the vertical and horizontal components of motion vectors, respectively.
- 7) Instead of embedding watermark bits in the magnitudes of the candidate motion vectors, Instead of embedding the data bit in the magnitude of motion vectors, the phase angle of two motion vectors is used for embedding watermark bits. The rule of embedding bits in the phases of motion vectors MV_2 and $MV_{2\pm 1}$, are written as follows:

The watermark bits are embedded in the following way:

If the embedding bit is 0, we need to have MV_2 , and $MV_{2\pm 1}$, such that:

$$0^\circ < |\theta_{2i} - \theta_{2i+1}| \leq 180^\circ, \text{ where } 0 \leq i \leq \lfloor \frac{n}{2} \rfloor \quad (1)$$

If the embedding bit is 1, we need to have MV_2 , and $MV_{2\pm 1}$, such that:

$$180^\circ < |\theta_{2i} - \theta_{2i+1}| \leq 360^\circ, \text{ where } 0 \leq i \leq \lfloor \frac{n}{2} \rfloor \quad (2)$$

If both the equations are not satisfied, then try the new motion vectors and continue until the entire watermark bits are embedded. The total angle i.e. $0^\circ - 360^\circ$ is divided into regions. These regions are defined in Tables II, III, and IV.

1 – bit – 2 regions area is used for watermark bit embedding as shown in Table II and Fig. 2. The 1 – bit – 2 region embedding can be extended to other multi-regions as shown in Tables III and IV. The whole range of 360° is divided into two regions where each region has range 180°. The watermark bits are embedded in the following way:

8) Compute the magnitude the motion vectors (MV) of the current frame that are obtained by using the Full-Search method.

9) Based on the pre-defined threshold T, select the set S for the candidate motion vectors (CMVs). $s = \{MV_0, MV_1, MV_2, \dots, MV_{n-1}\}, |S| = n$, where $(MV_{iV}^2 + MV_{iH}^2) \geq T, 0 \leq i < n$

10) Compute the phase angle of the CMV as: $\theta = \tan^{-1}(MV_{iV}/MV_{iH})$.

11) Select the pair of CMVs, MV_{2i} and $MV_{2i+1}, 0 \leq i < \lfloor \frac{n}{2} \rfloor$.

12) If the embedding bit is 0, then there are have two conditions.

a) If $0^\circ < |\theta_{2i} - \theta_{2i+1}| \leq 180^\circ$ then both the motion vectors will not be changed

b) If $180^\circ < |\theta_{2i} - \theta_{2i+1}| \leq 360^\circ$, then we will search for the new CMVs, MV'_{2i} and MV'_{2i+1} such that $|MV'_{2i}| \geq T$ and $0^\circ < |\theta'_{2i} - \theta_{2i+1}| \leq 180^\circ$ and $|MV'_{2i+1}| \geq T$ and $0^\circ < |\theta_{2i} - \theta'_{2i+1}| \leq 180^\circ$.

c) MSE_{2i} and MSE_{2i+1} are calculated. If $(MSE_{2i} < MSE_{2i+1})$, then replace MV_{2i} with MV'_{2i} , otherwise, replace MV_{2i+1} with MV'_{2i+1} .

13) If the embedding bit is 1, then there are two conditions again.

a) If $0^\circ < |\theta_{2i} - \theta_{2i+1}| \leq 180^\circ$ then both the motion vectors will not be changed.

b) If $180^\circ < |\theta_{2i} - \theta_{2i+1}| \leq 360^\circ$, then we will search for the new CMVs, MV'_{2i} and MV'_{2i+1} such that $|MV'_{2i}| \geq T$ and $180^\circ < |\theta'_{2i} - \theta_{2i+1}| \leq 360^\circ$ and $|MV'_{2i+1}| \geq T$ and $180^\circ < |\theta_{2i} - \theta'_{2i+1}| \leq 360^\circ$.

c) MSE_{2i} and MSE_{2i+1} are calculated. If $(MSE_{2i} < MSE_{2i+1})$, then replace MV_{2i} with MV'_{2i} , otherwise, replace MV_{2i+1} with MV'_{2i+1} .

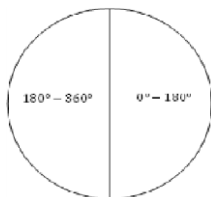


Fig. 2. 1 – bit – 2 Regions Embedding.

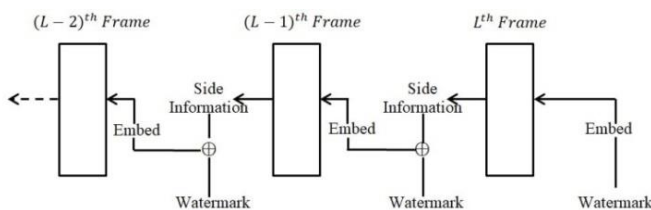


Fig. 3. Embedding Watermark Bits in the Motion Vectors of the Sequence Frames in the Reverse Order.

TABLE II. 1 – BIT – 2 REGIONS EMBEDDING

| | Phase Angle Range | Embedded Data |
|----------|-------------------|---------------|
| Region 1 | 0°~180° | 0 |
| Region 2 | 180°~360° | 1 |

TABLE III. 1 – BIT – 4 REGIONS EMBEDDING

| | Phase Angle Range | Embedded Data |
|----------|-------------------|---------------|
| Region 1 | 0°~90° | 0 |
| Region 2 | 90°~180° | 1 |
| Region 3 | 180°~270° | 0 |
| Region 4 | 270°~360° | 1 |

TABLE IV. 1 – BIT – 8 REGIONS EMBEDDING

| | Phase Angle Range | Embedded Data |
|----------|-------------------|---------------|
| Region 1 | 0°~45° | 0 |
| Region 2 | 45°~90° | 1 |
| Region 3 | 90°~135° | 0 |
| Region 4 | 135°~180° | 1 |
| Region 5 | 180°~225° | 0 |
| Region 6 | 225°~270° | 1 |
| Region 7 | 270°~315° | 0 |
| Region 8 | 315°~360° | 1 |

The embedding mechanism can be extended to *muti bit – multi Regions* embedding as shown in Table V.

TABLE V. 2 – BIT – 4 REGIONS EMBEDDING

| | Phase Angle Range | Embedded Data |
|----------|-------------------|---------------|
| Region 1 | 0°~90° | 00 |
| Region 2 | 90°~180° | 01 |
| Region 3 | 180°~270° | 11 |
| Region 4 | 270°~360° | 10 |

B. Side Information

For the exact recovery of the original frame on the extraction/verification side, side information along with the watermark bits are embedded. The side information is obtained during motion estimation and histogram modification steps. Motion vectors, boundary map and peak & zero point pairs are included in the side information. The number of motion vectors of a frame is

$$N(MV) = \frac{M \times N}{w \times h} \quad (3)$$

More motion vectors are recorded for the smaller blocks and vice versa. In the proposed scheme, the (16 × 16) block has been used. The other sizes of the block will be tested in the experiment. Overflow and underflow of the watermarked pixels are considered because of its use in the reconstruction of the frame. For example, the range of the pixel is (0 to 255) that can be modified to (-1 to 256). To avoid this issue, the authors in [10], proposed a pre-processing method where they find the zero point that is closed to the boundary i.e. (0 or 255), and the boundary pixels are removed and the pixels between the boundary pixels and zero points are

removed by modifying the histogram of the original frame. For histogram generating, the boundary pixels are not used and after embedding the watermark, new boundary pixels appear. Thus, the correct histogram can be obtained, while extracting the watermark on the verification side. In the proposed scheme, a binary vector is formulated to record all original boundary pixels that are assigned as 1, and pseudo boundary pixels that are assigned as 0. For most images or video frames, the length of the boundary map is very short or even zero. Side information along with the watermark bits are embedded in the previous frame. Similarly, the again the side information is generated and from the current frame and is combined with the watermark bits for embedding. The same procedure continues until we reach the first frame (embedding in the reverse order). The actually embedded data of a frame is given in Equation 4.

$$F'_i = \begin{cases} w_i, & i = L \\ si_i + w_i & 1 \leq i < L \end{cases} \quad (4)$$

where si represent side information and w represent original watermark bits. The ratio between the side information and the pure watermark capacity is shown in Table VI. As the block size is increased, then the side information decreased and vice versa. If the block size is decreased up to 4×4 , then a lot of side information is recorded and consequently, the imperceptibility will be highly affected. The block having size 16×16 have been used, where the side information is very low and increases the watermark strength by a maximum of four per cent. The threshold T is used while embedding the watermark that makes a tradeoff between the embedding capacity and imperceptibility.

C. Watermark Extraction

While extracting the embedded watermark from the frame, it must be ensured that the original frame and the corresponding reference frames are obtained. The extracting procedure along with recovering side information is shown in Fig. 4, which is the reverse of the order of the embedding procedure. All necessary information (reference frame and side information) for the extraction of embedded data can be prepared. Extracting the embedded watermark and recovering of the first frame employs the intra-frame approach, whereas all the other frames are processed by the inter-frame approach. After extracting the embedded information from the first frame i.e. F_1 , parse it to obtain pure watermark along with the side information that is used for extracting the embedded information from the frame F_2 . Similarly, after parsing the extracted data from F_2 , obtain the pure watermark and side information are obtained that are used for extracting the embedded information from the frame F_3 . This procedure continues until we reach the last frame.

TABLE VI. SIDE INFORMATION LENGTH FOR FRAMES

| | |
|--|--------|
| Number of motion vectors (One Frame) | 8100 |
| Total Frames | 168 |
| Boundary Map (average) | 2 |
| Side Information (Total) | 1856 |
| Watermark Capacity (Total) | 112224 |
| The ratio of side Information with watermark | 1.65% |

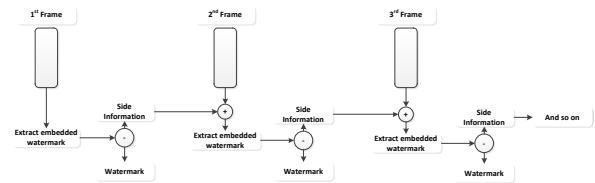


Fig. 4. Extraction of Watermark and Recovery of Side Information in the Order of Video Sequence.

Block diagram for extracting and restoring procedure for the original frame is shown in Fig. 5. Before extracting the F_i frame, we extract and restore the frame F_{i-1} to its original status. We continue the same procedure for all the frames to be extracted.

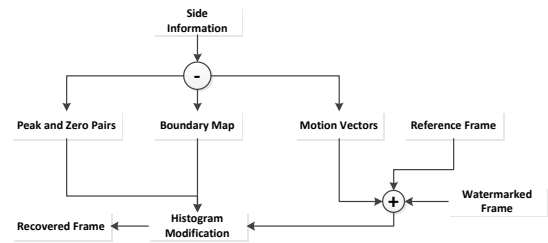


Fig. 5. Extracting and Restoring Procedure for the Original Frame.

V. EXPERIMENTAL RESULTS

MATLAB (2016a) environment has been used for the experimental results. The proposed method is applied to the ultrasound video. Watermark bits that contain the patient information are embedded. First, 1 – bit – 2 regions embedding is used and the results in terms of payload and PSNR are calculated as shown in Table VII. The payload varies according to the block size. In the experiments, 16×16 block is used and the watermark capacity is 112224. When the block size is reduced, i.e. 4×4 , then, the side information increased and hence the embedding watermark (Pure watermark and side information) strength increased. The payload mentioned in Table VII, is for four frames (frames number 7, 8, 9, 10). The capacity is measured in bits per block. In this work the capacity is $(8100 \times 4) \div 112220 = 0.29$.

TABLE VII. EXPERIMENTAL RESULTS, USING 1 – BIT – 2 REGIONS EMBEDDING

| Features | Details |
|--------------------------|--------------------------|
| Image sequence/video | Ultrasound video |
| Total Frames | 168 |
| Size | 1920 × 1080 |
| Aspect Ratio | 16:9 |
| Bits per Pixel | 24 |
| Frame Rate | 25 fps |
| Duration | 6.72 Seconds |
| Block Size | 16 × 16 |
| Total MVs (One Frame) | 8100 |
| T (Threshold) | 3 |
| Average CMVs (One Frame) | 668 |
| Payload | 112224 (For four Frames) |
| PSNR (Average) | 41dB |
| SSIM (Average) | 0.92 |

MATLAB environment has been used for the experimental results. A 6.72 seconds ultrasound sequence is chosen to test the proposed algorithm that contains 168 frames. Full-Search block-based motion estimation algorithm has been used to extract the motion vectors and then calculate the magnitude and phase angles of CMVs for embedding watermark bits. The four extracted frames (frame number 7, 8, 9, 10) are shown in Fig. 6.

As compared to the normal videos, the ultrasound image sequences have thousands of motion vectors as shown in Fig. 7. However, the highest magnitude of the motion vectors is 4.243, which is very low. The reason is that in the ultrasound video, the movement behaves like shrinking and expansion. The motion vectors of the four frames are shown in Fig. 7 and the corresponding watermarked motion vectors are shown in Fig. 8. As shown in Fig. 7, unlike the normal videos, the medical image sequences are more complex and are having thousands of motion vectors. Thus, the embedding capacity for watermark embedding is high and hence the reversible watermark that has high strength because of additional side information for reversibility can be embedded. The selection of suitable motion vectors is too easy because of many options.

In this paper, the ROI and RONI are not focused while embedding the watermark. Thus, for watermark embedding, it is too easy to select the high magnitude and phase angle in the motion vectors. Tackling of ROI and RONI is not easy without consulting the medical doctors and hospital management system.

Fig. 9 shows the watermarked frames (for frame number 7, 8, 9, and 10). In medical image applications, visual perception is very important, based on which the medical doctors decide. In the proposed scheme, the perceptual similarity (PSNR and SSIM) between the original and watermarked frames is much better and there is no problem for a doctor in diagnosis.

Performance comparison of the proposed technique with [6, 7, 32, 33] has been given in Table VIII. The comparison has been made with respect to several features like imperceptibility, watermark capacity, reversibility and ratio of extra side information with the pure watermark. In literature, several algorithms have been proposed to protect the ultrasound and other medical images but the reversible watermarking algorithms that specifically target the ultrasound image sequence were not found. For example, in [32], the authors have proposed to authenticate the ultrasound images using a compressed watermark. They are authenticating the images individually and they have not proposed the reversibility of the original image. Similarly, in [33], the authors have developed an algorithm for the security enhancement of medical videos. They are using motion vectors for watermark embedding but they are not targeting the ultrasound videos and have not mentioned anything for the reversibility of the original content. In this paper, the proposed approach is compared with the previous approaches [6, 7, 32, 33], where the authors are using normal/medical videos for embedding the watermarks /reversible-watermark(s). The experimental comparison shows that the proposed approach validates the usefulness of the reversible watermarking in

motion vectors for the protection of an ultrasound image sequence.

Fig. 10 shows the similarity of the watermarked image before transmission and the watermarked image received on the verification side. For this purpose, a Matlab function 'isequal' is used. It gives us the result logical 1 (True), because of the exact similarity. The similarity is checked by using the PSNR using Matlab function 'psnr'. The resultant show the Inf, which means the watermarked images on both the embedding and verification sides are identical. The watermarked frames number 7 and 8, before and after transmission are shown in Fig. 10, where the watermarked images are not attacked / tampered during the transmission. If the image is attacked, then the PSNR varies according to the strength of tampering or any other attack.

The table shows that the target is ultrasound image sequence/video for reversible watermarking, where the watermark bits are embedded in the motion compensation of the video. It can be seen that some of the papers did not provide the SSIM and hence it is difficult to analyze the structural similarity of the original and watermarked images properly. Just PSNR is not enough to measure the embedding distortion. The structural similarity of the watermarked images and videos must be checked.

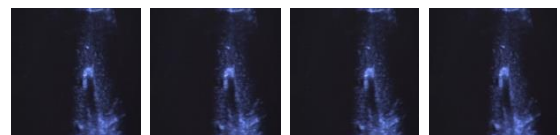


Fig. 6. Four Extracted Frames (Frames Number 7, 8, 9, 10) of the Ultrasound Video.

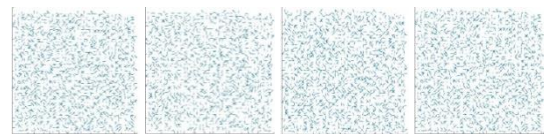


Fig. 7. The Motion Vectors of the Frames Given in Fig. 6.

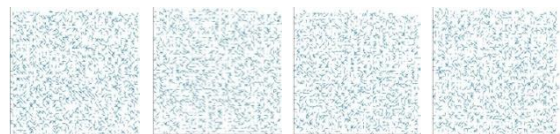


Fig. 8. The Watermark Embedded in the Motion Vectors of Fig. 3.

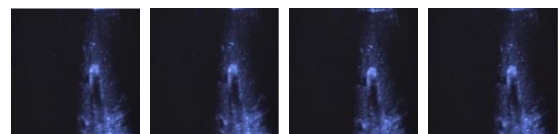


Fig. 9. Watermarked Frames (Frames Number 7, 8, 9, 10).

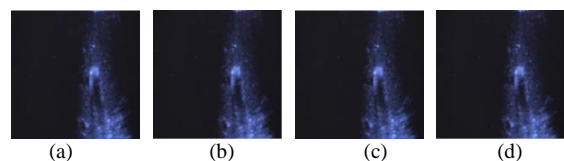


Fig. 10. (a~b) The Watermarked Frames before Transmission. (c~d) The Watermarked Frames after Transmission.

TABLE VIII. PERFORMANCE COMPARISON OF THE PROPOSED APPROACH WITH PREVIOUS APPROACHES

| Features | Vural <i>et al.</i> Ref. [6] | Vural <i>et al.</i> Ref. [7] | Badshah <i>et al.</i> Ref. [32] | Acharjee <i>et al.</i> Ref. [33] | Proposed |
|--|---|---|---|-------------------------------------|--------------------------|
| Video | Normal | Normal | Ultrasound Images | Medical Videos | Ultrasound video |
| Watermark | | | | Random | Patient Information |
| Watermark payload/capacity | High | High | Using Compressed watermark | Average | High |
| Side information | Yes | Yes | No | No | Yes |
| The ratio of side information with pure watermark | Not provided | 2.3% to 3.04 % | No | No | ≈ 1.65 % |
| Avoiding overflow/underflow | Do not tackle | Histogram modification | No | No | Histogram pre-processing |
| <i>Embedding in</i> motion vectors / spatial domain / frequency domain | Motion vectors | Motion vectors | Spatial domain | Motion Vectors | Motion vectors |
| Reversibility | Yes | Yes | No | No | Yes |
| PSNR between watermarked images on sender and receiver side | Not calculated | Not calculated | ≈ 50 dB (Highly compressed watermark) | ≈ 120 | Inf |
| PSNR between original and watermarked image | Better but decreases when watermark bit increases | Better but decreases when watermark bit increases | Not calculated | Not calculated | ≈ 41 db |
| SSIM | Not calculated | Not calculated | Not calculated | ≈ 0.97 | ≈ 0.92 |
| Robustness | Focusing on capacity and PSNR | Focusing on capacity and PSNR | Focusing on authentication and watermark recovery | Focusing on the recovered watermark | Semi-fragile |

In Table VIII, the second and third columns show that the PSNR is much better but when the authors increase the watermark capacity, the PSNR decrease to 30dB. Similarly in the PSNR and SSIM in the second last column are very high. The authors have calculated PSNR and SSIM between the watermarked images on the embedding and receiving side. In the proposed approach, the PSNR between the watermarked image before and after the transmission is Inf, which means that the images before and after transmission are identical. They did not measure the distortion of the original image after embedding the watermark bits. All other PSNRs and SSIMs, given in Table VIII are used to measure the performance of watermark strength and its embedding.

VI. CONCLUSIONS

In this paper, a reversible watermarking scheme has been proposed to secure the sequence of ultrasound video, wherein the original video can be retrieved. For reversibility, side information along with pure watermark is embedded. The side information is obtained from the motion vectors, boundary map and peak-and-zero point pairs. Watermark is embedded by modifying the magnitude and phase angles of the selected motion vectors, which ensures the low embedding distortion.

Extracting and recovering of the first frame employs the intra-frame approach, whereas all the other frames are processed by the inter-frame approach. After extracting from F1, the extracted data can be parsed to get pure watermark as well as side information used for extracting process of F2 and the procedure continues until we reach the last frame. Experimental results demonstrated that the proposed approach provides higher capacity and imperceptibility.

In future, an intelligent system can be used to select the most suitable motion vectors, which will enhance the security and visual quality of ultrasound videos.

VII. RESEARCH CONTRIBUTIONS AND LIMITATIONS

In the last two decades, several numbers of watermarking techniques have been proposed trying to come up with an efficient solution for securing the digital content especially medical data. The proposed scheme is able to protect the ultrasound sequence along with the recovery of the original sequence back. The proposed scheme is able to hide patient information as a watermark without affecting the visual perception of the watermarked sequence. In addition, the scheme is able to avoid the risk of a mismatch between patient information and its associated image/video.

Some limitations can be considered in future work. For example, if the block size is reduced, then a lot of side information is recorded and consequently, the imperceptibility will be highly affected. Similarly, in reversible watermarking, once the original image/sequence is restored then there will be no legal or ethical claim for the restored image. In addition, once the watermark is removed then the security of the image/sequence discontinues.

ACKNOWLEDGMENT

The author would like to thank Deanship of Scientific Research at Majmaah University for supporting this work under Project No. 1440-94.

REFERENCES

- [1] Nyeem, HMA., 2014. A digital watermarking framework with application to medical image security, PhD thesis, Queensland University of Technology.
- [2] Shih, F. Y., Zhong, X., Cheng, I., Satoh, CS., 2018. An adjustable-purpose image watermarking technique by particle swarm optimization, *Multimedia Tools and Applications*, 77, 1623–1642.
- [3] Saba, L., et al., 2016. Automated stratification of liver disease in ultrasound: An online accurate feature classification paradigm, *Computer Methods and Programs in Biomedicine*, Elsevier, 130, 118-134.
- [4] Borra et al. 2018. *Digital Image Watermarking: Theoretical and Computational Advances*, CRC Book.
- [5] Qasim, AF., Meziane, F., and Aspin, R., 2017. Digital watermarking: Applicability for developing trust in medical imaging workflows state of the art review, *Computer Science Review*, Elsevier, 27, 45-60.
- [6] Vural, C., and Barak, B., 2016. Adaptive reversible video watermarking based on motion-compensated prediction error expansion with pixel selection, *Signal, Image and Video Processing*, Springer, 10(7), 1225–1232.
- [7] Vural, C., and Barak, B., 2015. Reversible video watermarking using motion-compensated frame interpolation error expansion. *Signal, Image and Video Processing*, Springer, 9(7), 1613-1623.
- [8] Zhao, Z., Yu, N., and Li, X., 2003. A novel video watermarking scheme in compression domain based on fast motion estimation, *International Conference on Communication Technology*.
- [9] Li, Z., Zhao, J., Hu, J., and Tu, H., 2015. A reversible video steganography algorithm for MVC based on motion vector, *Multimedia Tools Applications*, 74(11), 3759–3782.
- [10] Zeng, X., Chen, Z-Y., Chen, M., and Xiong, Z., 2011. Reversible video watermarking using motion estimation and prediction error expansion, *Journal of Information Science and Engineering*, 27, 465-479.
- [11] Diljith M. T., and Jeffrey J. R., 2007. Expansion Embedding Techniques for Reversible Watermarking, *IEEE Transactions on Image Processing*, 16(3), 721-730.
- [12] Caldelli, R., Filippini, F., and Becarelli, R., 2010. Reversible Watermarking Techniques: An Overview and a Classification, *EURASIP Journal on Information Security*, 2010, 1-19.
- [13] Agilandeeswari, L., and Ganesan, K., 2016. A bi-directional associative memory based multiple image watermarking on cover video, *Multimedia Tools and Applications*, 75(12), 7211-7256.
- [14] Loganathan, A., and Kaliyaperumal, G., 2016. An adaptive HVS based video watermarking scheme for multiple watermarks using BAM neural networks and fuzzy inference system, *Expert Systems with Applications*, 63, 412-434.
- [15] Agilandeeswari, L., Ganesan, K., 2018. RST invariant robust video watermarking algorithm using quaternion curvelet transform, *Multimedia Tools and Applications*, 77(19), 25431-25474.
- [16] Dey, N., et al. 2013. DWT-DCT-SVD based intravascular ultrasound video watermarking, *World Congress on Information and Communication Technologies*, India.
- [17] Naheed, T., Usman, I., Khan, TM., Dar, AH., and Shafique, MF., 2014. Intelligent reversible watermarking technique in medical images using GA and PSO, *Optik - International Journal for Light and Electron Optics*, Elsevier, 125, 2515-2525.
- [18] Lei, B., Tan, E-L., Chen, S., Ni, D., Wanga, T., and Lei, H., 2014. Reversible watermarking scheme for medical image based on differential evolution, *Expert Systems with Applications*, Elsevier, 41, 3178-3188.
- [19] Acharjee, S., Chakraborty, S., Ray, R., and Nath, S., 2014. Watermarking in motion vector for security enhancement of medical videos, *International Conference on Control, Instrumentation, Communication and Computational Technologies*, 589-594.
- [20] Yeh, H-L., Gue, S-T., Tsai, P., and Shih, W-K., 2014. Reversible video data hiding using neighbouring similarity, *IET Signal Processing*, 8(6), 579-587.
- [21] Niu, K., Yang, X., Zhang, and Y., 2017. Novel Video Reversible Data Hiding Algorithm Using Motion Vector for H.264/AVC, in *Tsinghua Science and Technology*, 22(5), 489-498.
- [22] Arsalan, M., Qureshi, AS, Khan, A., and Rajarajan, M., 2017. Protection of medical images and patient-related information in health care: Using an intelligent and reversible watermarking technique, *Applied Soft Computing*, Elsevier, 51, 168-179.
- [23] Vural, C., and Yıldırım, I., 2017. Reversible video watermarking through recursive histogram modification, *Multimedia Tools and Applications*, 76, 15513-15534.
- [24] H.-Y. Ding, Y. Zhou, Y. Yang and R. Zhang, "Robust blind video watermark algorithm in transform domain combining with 3D video correlation," *Journal of Multimedia*, vol. 8, no. 2, pp. 161-167, 2013.
- [25] O. S.Faragallah, "Efficient video watermarking based on singular value decomposition in the discrete wavelet transform domain," *AEU: International Journal of Electronics and Communication*, vol. 67, no. 3, pp. 189-196, March 2013.
- [26] W. Yu, D. Hu, N. Tian and Z. Zhou, "A novel search method based on artificial bee colony algorithm for block motion estimation," *EURASIP Journal on Image and Video Processing*, vol. 2017, no. 66, pp. 1-14, 2017.
- [27] M. S. A. K. and A. Ali, "Multiresolution video watermarking algorithm exploiting the block-based motion estimation,," *Journal of Information Security*, vol. 7, no. 4, pp. 260-268, July 2016.
- [28] T. Bernatin and G. Sundari, "Comparative analysis of different diamond search algorithms for block matching in motion estimation,," *ARNP Journal of Engineering and Applied Sciences*, vol. 12, no. 11, pp. 3550-3553, 2017.
- [29] M. Jakubowski and G. Pastuszak, "Block-based motion estimation algorithms—a survey,," *OPTO–Electronics Review*, vol. 21, no. 1, pp. 86-102, 2013.
- [30] S. P. Metkar and S. N. Talbar, "Fast motion estimation using modified orthogonal search algorithm for video compression,," *Signal, Image and Video Processing*, vol. 4, no. 1, pp. 123-128, 2010.
- [31] Gunnarsson, E, <https://www.videvo.net/video/ultrasoundscan-5/3306/>.
- [32] Badshah, G., Liew, S-C., Zain, J M., and Ali, M., 2016. Watermarking of ultrasound medical images in teleradiology using compressed watermark, *Journal of Medical Imaging, SPIE*, 3(1), 170011-170019.
- [33] Acharjee, S., Ray, R., Chakraborty, S., Nath, S., Dey, N., 2014. Watermarking in Motion Vector for Security Enhancement of Medical Videos, *International Conference on Control, Instrumentation, Communication and Computational Technologies (ICCICCT)*, 589-594.